Published by :
http://www.ijert.org

International Journal of Engineering Research & Technology (IJERT)
ISSN: 2278-0181
Vol. 12 Issue 07, July-2023

Failure Prediction using Acoustic Emissions and Artificial Neural Networks

Karthik Bujuru
R&D Engineer,
Irvine, CA USA

V. Malolan
Scientist,
Advanced Systems Laboratory,
DRDO, Hyderabad, India

Abstract **- Quality assessment of structural integrity of critical systems such as Rocket motor casings is challenging and lacks adequate methods. There have been attempts to ascertain the failure loads of structures made from composite materials, but limited research was performed using metals like maraging steels. 17 dog-bone shaped 18Ni maraging steel (Grade 250) specimens were subjected to monotonic loading to collect tensile test data in the form of acoustic emissions (AE). This AE data was preprocessed and filtered to signal parameters that can be used to train back-propagation multi-layer perceptron (MLP) neural network, specifically using amplitude-hit, Weibull distribution parameters and energy/hit rates. The training and prediction were conducted at various levels of 25% to 90% of the failure loads and was determined that the model was able to predict the failure load at proof loads as low as 50% with minimal prediction error of 4.5%. The results indicate that an accurate failure prediction may be achieved using indirect method of training the artificial neural networks using acoustic emissions data from specimens under load. Thus, acoustic emissions and artificial neural networks pave the way for online monitoring of structural integrity of critical systems such as rocket motors used in satellite launch vehicles at loads much lower than the failure load.**

Keywords— Acoustic Emissions, Artificial Neural Networks, Material failure prediction, Non-destructive techniques

I. INTRODUCTION

Rocket motor casings are significant subsystems for satellite launch vehicles and are necessary to be realized with materials that withstand high thermal loads, structural loads, possess high creep resistance and specific strength[1]. Besides these criteria, material selection also needs to focus on aspects such as modes of failure and fabrication requirements. Table 1 lists the properties of typical materials commonly used for solid rocket motor casings. The 18% Nickel maraging steels are advantageous over the other alloys for their good forming, forging characteristics, their ability to be heat treated at low temperatures, dimensional stability during age hardening, higher fracture toughness and the ability to be machined in soft condition with minimum distortion[2]. However, these high strength maraging steel materials can undergo premature brittle fractures at stress levels lower than the designed limits due to stress concentration around inherent material defects like voids and the defects induced during the fabrication processes. These defects could reduce the material's fracture toughness which requires the designers to follow fracture-based design methodology and be more dependent on the quality control strategy. Typical NDT techniques involved in the inspection of rocket motor casings for defect detection include liquid penetrant inspection, ultrasonic inspection, radiographic inspection, and acoustic emission inspection. While each of these NDT techniques is more or less better suited for a given application, this paper is focused on investigating the use of acoustic emissions as an NDT tool to evaluate the structural integrity of rocket motor casings made from maraging steel using artificial neural network.

Table 1 Comparative Mechanical Properties of Various Alloys

Material	*Design Yield Strength, MPa*	*Modulus of Elasticity, GPa*	*Density Gm/cc*	*Heat Treatment*
Low Alloy Steel 4130 4335V D6aC 15CDV6	1035-1240 1240-1380 1240-1660 1080-1280	199.95 199.95 199.95 199.95	7.83 7.83 7.83 7.83	Quench and Temper
Maraging Steel Grade 200 Grade 250 Grade 300	1380 1660 1930	189.61 189.61 189.61	8.00 8.00 8.00	Solution Anneal and age
Titanium Ti-6Al-4V	1035	110.32	4.62	Solution Anneal and age

A. Acoustic Emissions

Acoustic emissions are transient elastic waves that are generated by rapid release of energy from localized sources within a material when it is stressed[3]. This NDT is a fast-maturing technique to play an effective role in real time monitoring of the active defects in structures similar to rocket motor casings. The AE technique identifies severity of the defects in the material by quantitatively assessing high energy emissions that are characterized by high amplitude and long duration events[4]. The low displacement high frequency mechanical shock wave signals produced by the acoustic emissions are received by the piezo-electric sensors placed on the material and are converted into suitably amplified electronic signal. Most of the emission sources can be distinguished by their acoustic emission signature. The extent of AE activity is minimal under 50% of the failure load, and increases with

International Journal of Engineering Research & Technology (IJERT)
ISSN: 2278-0181
Vol. 12 Issue 07, July-2023

increasing load depending on presence of the material defects. These acoustic emissions are correlated with the actual straining of the material, and allow for characterizing the material for yield and ultimate tensile strengths[5]. Mechanical behavior of the material can be correlated to AE attributes such as amplitude, counts, energy rise time, duration, hit rate, energy rate, and amplitude-hit distribution plots[6],[7].

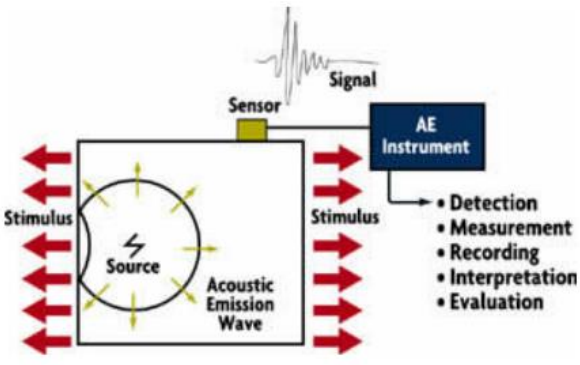

Figure 1 Process of AE Generation

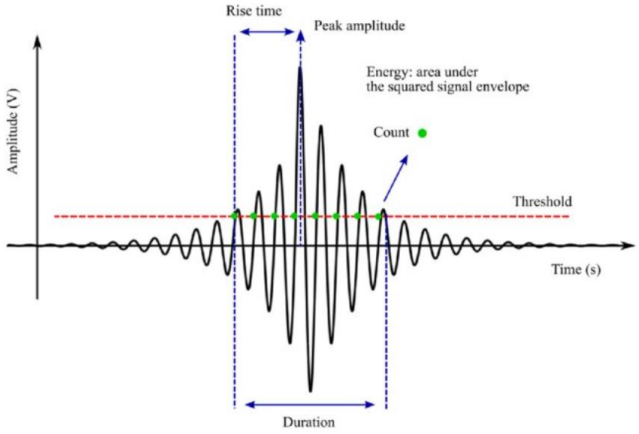

Figure 2 Typical AE Wave

B. Artificial Neural Networks

Artificial neural network-which has proximity to biological neural network-is an adaptive computer program or an iterative numerical technique that facilitates solutions to problems such as prediction and classification of data. The relationship between inputs and outputs is established through a training process in which a set of inputs are processed through the neural network to obtain outputs which are compared to the known correct values. The errors in the network outputs are minimized to an acceptable level through an iterative process of modifying the network parameters.

Typical artificial neurons have certain parameters such as bias/threshold, transfer function and synaptic weights. The weighted signals from synapse get combined linearly in the adder along with bias. The output from the adder is processed through transfer functions (excitatory or inhibitory) such as sigmoid, threshold, hard limiter etc. to alter the amplitude of the output of the neuron.

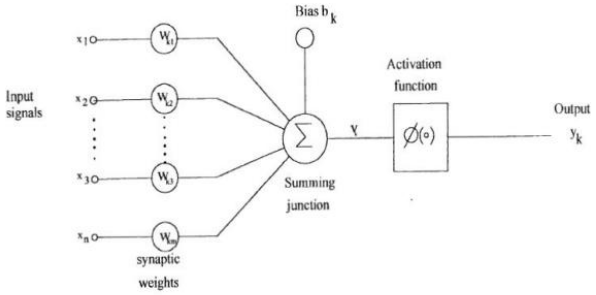

Figure 3 Architecture of Artificial Neuron

A multilayer perceptron (MLP) neural network has a single input layer, one or more hidden layers, and one output layer. The signal propagates through the neural network layer by layer, while undergoing training utilizing error back-propagation (BP) algorithm to adjust the synaptic weights based on the difference between the outputs and the desired response[8]. The hidden layers of the error-back propagation algorithm analyze the inter-nodal relationship from the input layer-otherwise referred to as feature, and allows for more abstract representation of the input information in the hidden layers[9]. This ability of the BP network allows for recognition of features in complex patterns with adequate training [10].

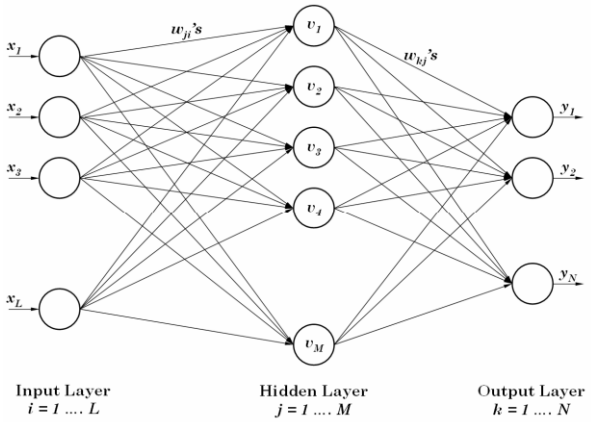

Figure 4 Back Propagation Multi-Layer Perceptron

II. EXPERIMENTAL SETUP

This section discusses the experimental setup and the procedure that was used to tensile test the specimens; collect, and process the acoustic emission data, train the ANN program with acoustic data, and utilize the trained model to predict the peak load outcomes of test samples. The 18% nickel maraging steel dog-bone shaped samples tested for this study are presented in Figures 6. Of the seventeen (17) samples a set of 9 specimens had simulated cracks (notches), another set of 1 specimen had weld defect and the last set of 7 specimens were defect free. The samples with notches were fabricated with 3 different kinds as noted in AMS 2632A standard and listed in Table 2.

International Journal of Engineering Research & Technology (IJERT)
ISSN: 2278-0181
Vol. 12 Issue 07, July-2023

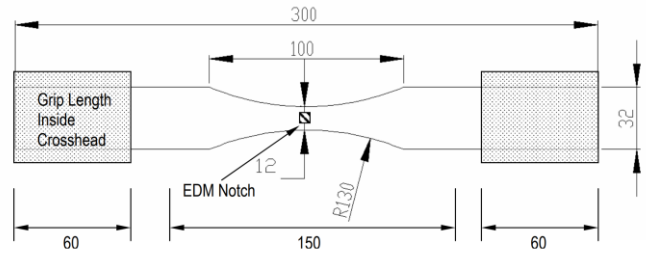

Figure 5 Drawing of specimen showing critical dimensions

The notches designed were per ultrasonic inspection standard AMS 2632A which specifies 3 different kinds- E, F and G. These samples are tested in Walter-Bai hydraulic servo system to collect the tensile data while the piezo-electric sensors on the samples also collect AE data while under load. The AE data from the test samples is routed through the data acquisition system, the test setup for which is detailed in the next section.

A. AE Monitoring and Data Acquisition System

The Physical Acoustics corporation (PAC) AEWin system was used for this study. The system records the initiation and growth of the defects and noise in the specimens under test in the form of transient waveform, to analyze store and display the resulting data. The main components of the AE system include an IBM compatible personal computer, six AE-DSP-32/16 boards, the MISTRAS software (Graphical User Interface (GUI) software) for data acquisition and display. The other miscellaneous components include acoustic sensors, plug-in filters, and connecting cables.

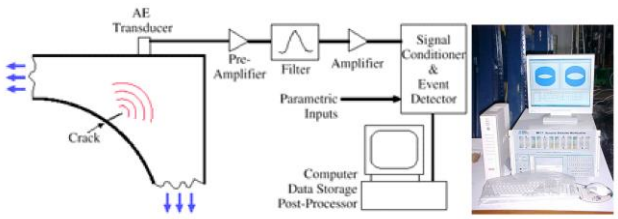

Figure 6 Schematic Block Diagram of AE-Win System

PAC's MICRO 30D sensitive piezo-electric sensors with operating bandwidth between 100-500KHz were fixed on the specimen's surface using adhesive tapes to receive acoustic emissions related to damage growth and noise during the testing. These AE signals from the transducers, which are of the order of a few millivolts, are fed into a preamplifier and then into a plug-in filter with a bandpass of 100 KHZ- 1.2 MHz to filter out the noises related to oil flow in actuator assembly, hydraulic grips, friction, and vibrational energy etc. from the fixture accessories. The amplified and filtered output from the amplifier, which is in an order of few volts, is fed into AE-DSP-32/16 board which under software control is used to filter the data to the required level. The filtered signal is then processed in AE-DSP-32/16 board into outputs containing the required AE signal features that are footprint of the defects in the specimen.

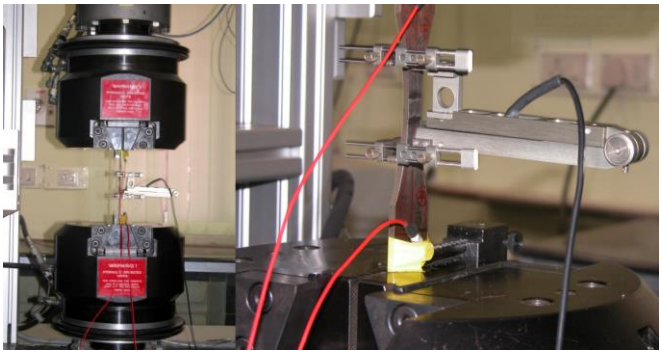

Figure 7 Test specimen setup in Walter-Bai Hydraulic Tester

III. RESULTS AND DISCUSSION

Table 2 details the data from 17 test samples that were subjected to tensile loading up to failure using the test setup discussed in section 3. The differences in test samples such as weld thickness, failures in heat affected zones (HAZ) and behavior of different notches led to a difference of 21% in the failure loads in the specimens. The lowest failure load was 70.5 KN and the highest was 84.8 KN. The AE data collected from the specimens is analyzed using AE-Win system and MITRAS signal data acquisition and analysis software.

Figure 8 Actual samples manufactured and tested

Table 2 Test Sample defect type, failure mode and Peak Load

Specimen	*Type of Defect*	*Type of failure observed*	*Failure Load in KN*
Specimen 10	Weld Defect	Defect failure	70.57
Specimen 05	G-Notch	Notch failure	74.79
Specimen 23	70% G-Notch	Notch failure	72.47
Specimen 22	70% G-Notch	Notch failure	75.30
Specimen 03	50% G-Notch	Notch failure	79.13
Specimen 20	50% G-Notch	Notch failure	79.14
Specimen 06	F-Notch	Notch failure	79.47
Specimen 17	F-Notch	Notch failure	80.91
Specimen 14	E-Notch	HAZ failure	84.85
Specimen 24	None	Weldment failure	79.84
Specimen 07	None	Weldment failure	80.27
Specimen 01	None	Weldment failure	80.56
Specimen 13	None	Weldment failure	80.81
Specimen 11	None	Weldment failure	75.80
Specimen 04	None	Weldment failure	81.43
Specimen 18	None	HAZ failure	81.54
Specimen 08	None	HAZ failure	82.79

A. Neural Network Program Training

The different characteristics of failure mechanism or defect of the specimen correspond to different kinds of AE signals and their signal parameters. The neural network program is required to be adequately trained with relevant data for

International Journal of Engineering Research & Technology (IJERT)
ISSN: 2278-0181
Vol. 12 Issue 07, July-2023

allowing it to generate prediction equations for an accurate defect classification and predict impending failure.

Signal parameters such as cumulative AE activity, AE hit rate, AE energy rate, AE count rate were assessed for their fit to be used as inputs to ANN to accurately predict the failure loads. These parameters, when interposed with stress-strain graph were able to accurately predict the onset of yielding but were unable to predict the impending failure with the required accuracy. Therefore, these parameters were used as augmented input to the neural networks program for failure prediction. Other signal parameters such as the AE amplitude distribution data (Figure 8) are shown to contain information specific to identification of failure mechanisms in materials [13]. Various failure mechanisms have characteristic humps or bands in amplitude distribution with distinctive differences between failure mechanisms for plastic deformation and crack propagation. A relatively large number of hits at high peak amplitude indicates a high-quality part while small number of hits at low peak amplitude indicates part with defects.

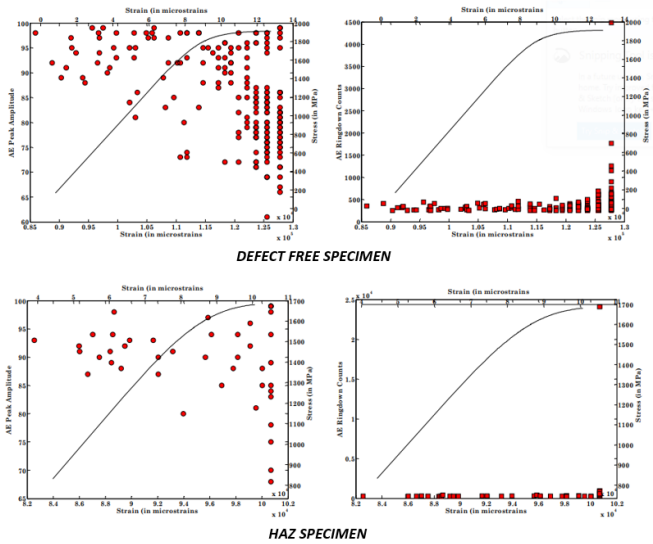

Figure 9 Filtered AE data and Stress-strain comparative plot

The same amplitude-hit distribution data, when modeled using Weibull distribution yields 3 parameters (A0, θ and b) identifying the shape of the distribution. A0 represents threshold amplitude, θ represents mean of amplitude distribution which represents ductility or brittleness of the specimen, and b represents skewness of distribution towards low or high stress events with high value of b representing high quality part. Once these Weibull parameters for the amplitude-hit distribution are identified, they were used as inputs for the neural network model for failure prediction.

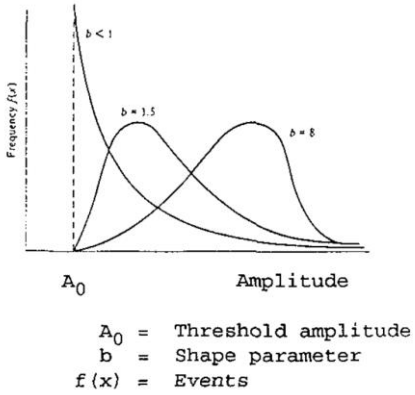

Figure 10 Weibull distribution and their parameters effect on shape of distribution

Of the 17 specimens, 2 specimens (11 and 23) were excluded from training or testing due to their slippage from the grips. For MLP training, unique amplitude-hit distribution data sets of 7 specimens were selected as a training set. 8 of the remaining specimens were used to test the trained MLP network.

Table 3 Specimens used for Training

Specimen	*Type of Defect*	*Type of failure observed*
Specimen 10	Weld Defect	Defect Failure
Specimen 05	G-Notch	Notch Failure
Specimen 22	70% G-Notch	Notch Failure
Specimen 17	F-Notch	Notch Failure
Specimen 14	E-Notch	HAZ Failure
Specimen 07	None	Weldment Failure
Specimen 01	None	Weldment Failure

A total of 60 amplitude distributions were used as inputs for training while adopting methods to make the network faster and efficient. Other inputs such as hit rate, energy rate and count rates were also used as augmented inputs for training. Other statistical parameters from amplitude Weibull distribution were also used as inputs. In total there were 65 distinct inputs and corresponding AE hit distribution that were used as input to the neural network. One specific or a combination of parameters was used to create multiple MLP programs with each trained differently from the other. A significant number of trial-and-error methods were adopted to determine the network parameters such as nodes in the hidden layer, changes in learning rate, minimization of weights initiated using random numbers etc.

Table 4 Characteristics of MLP Neural Network

Feature	*MLP Network Architecture*
Architecture	Input Layer-single hidden layer-output layer
No. of Input Nodes	65
No. of output Nodes	1 (tracked failure load)
No. of hidden nodes	8
Bias Level	Randomly initiated (less than 1)
Presentation of training data	Sequential
Training error representation	Mean square error
Weight Initiation	Small and randomly selected
Learning rate	0.1
Activation function	Sigmoidal
Criteria for stopping	Acceptable error level
Learning mode algorithm	Supervised-error back propagation
Programming language	MATLAB
Platform for simulation	Win32, Intel

International Journal of Engineering Research & Technology (IJERT)
ISSN: 2278-0181
Vol. 12 Issue 07, July-2023

B. *Failure Prediction using Neural Networks*

Two sets of prediction exercises were conducted. In one, only hit-amplitude distribution data (60 inputs) trained model was used. The predictions for failure load using this particular type of trained model were conducted at 50% of failure loading. The resulting error when a comparison between the model predicted values and the actual values of failure loading were made was 8.1%. In the second set of prediction exercises, the model trained with 65 inputs which include amplitude distribution data along with rate inputs and Weibull distribution parameter inputs was used. The predictions using this trained model resulted in a reduction of the error to 4.5%. Therefore, it was established that using augmented inputs to the neural network model reduced the error by half.

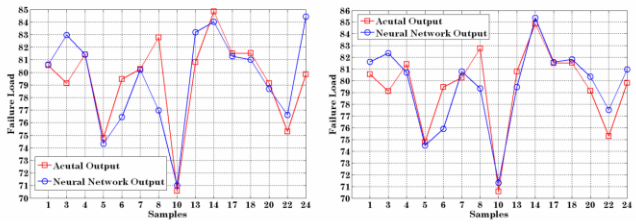

(a) Hit-Amplitude Distribution Only (b) Augmented inputs (65)

Figure 11 Comparison between 60 inputs and 65 inputs

The developed and optimized neural network was trained with 7 specimens and tested for the full set of specimen's data at various load levels starting from 25% to 90% and outputs were compared to that of the actual failure loads

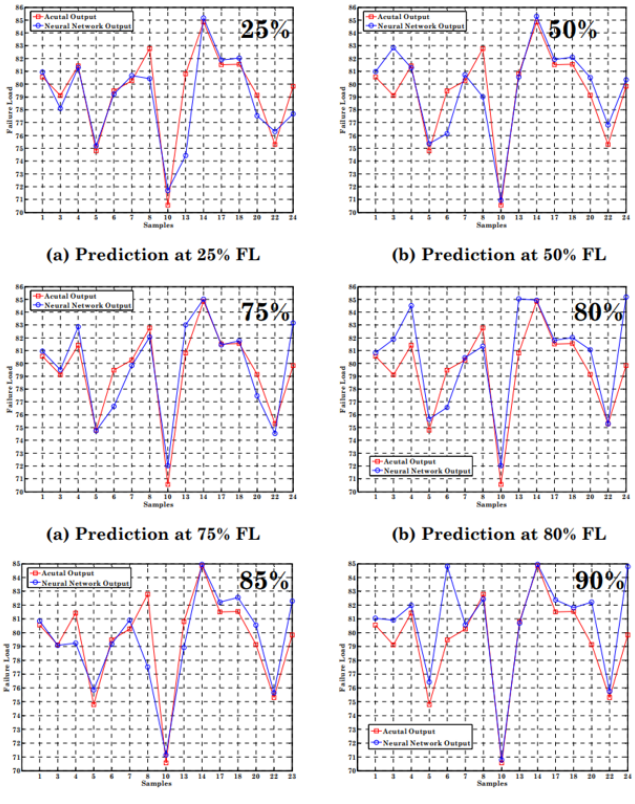

(a) Prediction at 25% FL (b) Prediction at 50% FL

(a) Prediction at 75% FL (b) Prediction at 80% FL

(a) Prediction at 85% FL (b) Prediction at 90% FL

Figure 12 Comparison of NN output with Actual failure loads

Table 5 Prediction Errors at various load levels

Specimen	*Percentage error in prediction at 25%*	*Percentage error in prediction at 25%*	*Percentage error in prediction at 25%*	*Percentage error in prediction at 25%*	*Percentage error in prediction at 25%*	*Percentage error in prediction at 25%*
Specimen 01	0.4781	0.529	0.49768	0.33887	0.35551	0.61797
Specimen 03	-1.3028	4.6939	0.47771	3.4761	-0.05784	2.2369
Specimen 04	-0.16647	-0.19034	1.75	3.7853	-2.6817	0.67171
Specimen 05	0.53805	0.75892	-0.07098	1.1437	1.4404	2.1828
Specimen 06	-0.31876	-4.1823	-3.5542	-3.6702	-0.36069	6.7083
Specimen 07	0.48845	0.55624	-0.52608	0.22711	0.80379	0.36491
Specimen 08	-2.8563	-4.5602	-0.86636	-1.7564	-6.3514	-0.43028
Specimen 10	1.6174	0.52251	2.0623	2.0429	0.82245	0.30116
Specimen 13	-7.8922	-0.30505	2.7199	5.2497	-2.3148	-0.14371
Specimen 14	0.36403	0.53194	0.18995	0.086295	0.10919	0.12843
Specimen 17	0.4767	0.52389	-0.06868	0.36897	0.88839	1.0814
Specimen 18	0.59641	0.67763	0.27913	0.58859	1.2304	0.33254
Specimen 20	-2.035	1.7254	-2.1074	2.4372	1.7897	3.8889
Specimen 22	1.3404	2.0147	-1.0069	-0.01225	0.45596	0.61185
Specimen 14	-2.6907	0.6342	4.1527	6.7059	3.0786	6.2185
No. of cycles	26677	24617	25312	42108	19521	68037

From table 5, it is evident that the neural network model's prediction error is at 7.9% when the proof load ranges is between 25% to 90%. But considering that acoustic emissions are negligible during the initial phase of loading at 25%, and when the proof loading range of 50-90% range is considered, the prediction error is reduced to 6.7%. However, the grip and slip noises are highest when the proof loading percentages are in 80-90% range. Therefore, if the loading ranges are changed to 50-75% of the failure load, the prediction error of the model is reduced to 4.5%. This allows for predicting failure load of specimen effectively at loads as low as 50% of failure load with reasonable prediction error. This confirms that the use of augmented input, i.e., rate values and Weibull parameters along with the hit-amplitude distribution data reduced the prediction error.

IV. CONCLUSION

The acoustic emission data from the 15 specimens (2 specimens excluded from analysis due to slippage) was used to train and test back-propagation multi-layer perceptron neural network at 25%, 50%, 75%, 80% and 90% of failure load. The results indicate that the neural network model was able to accurately predict the failure load at proof loads as low as 50% with 4.5% prediction error. It was also identified that the augmented input to the neural network like hit/energy rate and Weibull distribution parameters as training parameters have reduced the prediction error by 4%. Also, the model was able to appropriately segregate grip noise data from the aggregate data set when specimens were loaded to 80-90% of proof loads by adjusting the synaptic weights without having to remove it manually. The research presented in this paper substantiates the feasibility of using neural networks and non-destructive techniques such as acoustic emission testing data to confirm accurate failure load prediction. However, extending this research for developing an online structural integrity monitoring system requires additional analysis and further understanding of

International Journal of Engineering Research & Technology (IJERT)
ISSN: 2278-0181
Vol. 12 Issue 07, July-2023

influence of material properties, heat treatment conditions, acoustic wave propagation effects like reflection, actual test parameters and actual field conditions.

ACKNOWLEDGMENT

This paper is based on the extensive work conducted by the esteemed scientist V. Malolan at Advanced Systems Labs located in Hyderabad, India.

REFERENCES

[1] ASM Handbook Committee, *Properties and Selection: Irons, Steels, and High-Performance Alloys*, vol. 1. ASM International, 1990. doi: 10.31399/asm.hb.v01.9781627081610.

[2] D. P. M. da Fonseca, A. L. M. Feitosa, L. G. de Carvalho, R. L. Plaut, and A. F. Padilha, "A Short Review on Ultra-High-Strength Maraging Steels and Future Perspectives," *Materials Research*, vol. 24, no. 1, 2021, doi: 10.1590/1980-5373-mr-2020-0470.

[3] D. G. Aggelis *et al.*, "Acoustic Emission," 2021, pp. 175–217. doi: 10.1007/978-3-030-72192-3_7.

[4] American Society of Non-destructive Testing, *Nondestructive Testing Handbook, Vol. 6: Acoustic Emission Testing (AE), 3rd ed.* American Society of Non-destructive Testing, 2005.

[5] L. L. L. and J. L. T. N. O. Gross, "Acoustic Emission Testing of Pressure vessels for Petroleum Refiners and Chemical Plants," in *Acoustic Emissions*, 1972, pp. 270–296.

[6] T. Chelladurai, A. S. Sankaranarayanan, A. R. Acharya, and R. Krishnamurthy, "Acoustic emission response of 18% Ni Maraging steel weldment with inserted cracks of varying depth to thickness ratio," *Mater Eval*, vol. 53, no. 6, 1995.

[7] American Society for Testing and Materials, "ASTM E569-02, Standard Practice for Acoustic Emission Monitoring of Structures During Controlled Simulation," 2020.

[8] D. E. Rumelhart, G. E. Hinton, and R. J. Williams, "Learning representations by back-propagating errors," *Nature*, vol. 323, no. 6088, pp. 533–536, Oct. 1986, doi: 10.1038/323533a0.

[9] B. D. Ripley, *Pattern Recognition and Neural Networks*. Cambridge University Press, 1996. doi: 10.1017/CBO9780511812651.

[10] W. S. Sarle, "' Neural Network FAQ', Part 1 - 7, Introduction, Periodic, Posting to the Usenet newsgroup comp.ai.neural-nets," *ftp://ftp.sas.com/pub/neural/fa.html*.

[11] T. Tsukikawa *et al.*, "Acoustic Emission Testing During a Burst Test of a Thick-Walled 2-1/4 Cr-1 Mo Steel Pressure Vessel," *J Press Vessel Technol*, vol. 102, no. 4, pp. 353–362, Nov. 1980, doi: 10.1115/1.3263345.

[12] E. V. K. W. I. J. L. R. G. H. Hill, "Burst pressure prediction in graphite/epoxy pressure vessels using neural networks and acoustic emission amplitude data," *Mater Eval*, vol. 54, no. 6, Jun. 1996.

[13] R. K. P. R. N. A. R. A. T. Chelladurai, "Microstructure studies on M250 Maraging steel weldments in relation to acoustic emission," in *Trends in NDE Science & Technology; Proceedings of the 14th World Conference on Non-Destructive Testing*, New Delhi: Ashgate Publishing company, Dec. 1996, pp. 2399–2404.